Soil Dynamics and Earthquake Engineering 177 (2024) 108401

Contents lists available at ScienceDirect

Soil Dynamics and Earthquake Engineering

journal homepage: www.elsevier.com/locate/soildyn

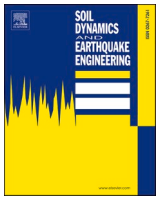

Correlations between p-wave velocity and *SPT-N* for saturated and unsaturated alluvial clays using dimensional analysis

Santiago Ortiz-Palacio [a], Sergio J. Ibanez [a,*], Diego Sancho [b], Jose Angel Porres [a]

[a] Department of Geotechnical Engineering, University of Burgos, Burgos, Spain
[b] Doctoral School, University of Burgos, Burgos, Spain

ARTICLE INFO

Original content: New correlations between Vp and SPT-N-Research data (Original data)

Keywords:
p-wave
SPT-N
Dimensional analysis

ABSTRACT

The aim of this research is to establish practical and robust correlations between dilatational wave velocities (p-wave velocities, V_p) and the Standard Penetration Test blow count (*SPT-N*). Very low levels of correlation are recorded with the conventional single variable approaches, in consequence, a multivariable study is needed for higher precision. A dimensional analysis was conducted including other soil parameters that condition this physical phenomenon, such as the void ratio (e), the degree of saturation (S_r), the effective overburden pressure (σ'_v), and the particle density (γ_s), for greater precision with V_p and *SPT-N* correlations. Over 100 seismic and SPT tests were performed around the coastal city of Juchitán de Zaragoza (Oaxaca), Mexico, to gather information for this research. As a result, two dimensionless indexes -DSI_u (Undrained Dilatational Stiffness Index) and $MDSI_u$ (Modified Undrained Dilatational Stiffness Index)- yielded two alternative expressions between both indexes and V_p. In this way, a strong relationship between V_p and *SPT-N* was obtained with an adjusted coefficient of determination R^2 value of 0.93.

1. Introduction

1.1. State of the art

Seismic surveying is increasingly used as a convenient technique for measuring the mechanical properties of soil [1,2] in new research that is focused on the links between stress-strain behaviour and critical failure in soils.

Dilatational, primary or p-wave velocity (V_p) and shear, secondary, or s-wave velocity (V_s) figure among the most important seismic parameters [1].

In essence, seismic geophysics is a useful, powerful, and relatively inexpensive instrument for geotechnical surveying, even though, as with every technique, it has both a specific field of use and usage constraints, *e.g.*, deposits in which soft layers are hidden between stiffer strata [3] (although any soft layers can be located through the use of complementary geophysical tests, such as electrical resistivity).

On the other hand, the research of many authors has been concentrated on the Standard Penetration Test-Blow Count (*SPT-N)* as the key to setting the parameters that can best predict the shear strength of soils. While hardly the most practical and accurate method when compared with well-programmed laboratory testing of undisturbed specimens [4], the *SPT-N* nevertheless meets four important requirements for research projects on soil mechanics: easy performance, fast-paced resolution meeting tight deadlines, cost-effectiveness, and the constraints on equipment availability found in underdeveloped and developing socio-economic settings.

Any statistically fitted relationship between the *SPT-N* and the soil strength or stiffness will have a significant uncertainty when based on a single variable approach, so it will be improved when other soil properties are included in the analysis. Moderate uncertainty has, for example, been associated with Standard Penetration Test (*SPT*) results [4,5] that offer estimates of the angle of internal friction in cohesionless soils [4,6–8] and the relative density of soils [9–11]. Likewise, the connection between the *SPT-N* and the undrained shear strength of a given soil have been described in investigations on fine-grained soils [12,13], and in some other studies that also included the influence of soil plasticity [14,15]. While these relations have traditionally been identified as rough [7] or not applicable [16], new multivariable studies have emerged to obtain better correlation results for cohesive soils (through traditional regression treatments and using Artificial Neural Networks), some of which with promising results [17,18].

* Corresponding author. Department of Geotechnical Engineering, University of Burgos, Escuela Politécnica Superior, Campus San Amaro, Calle Villadiego s/n, 09007, Burgos, Spain.
E-mail address: sibanez@ubu.es (S.J. Ibanez).

https://doi.org/10.1016/j.soildyn.2023.108401
Received 8 July 2023; Received in revised form 16 October 2023; Accepted 4 December 2023
Available online 12 December 2023

1.1.1. V_s - SPT-N existing correlations

Over the past few decades, many empirical studies have been focused on the relationship between shear wave velocity and the *SPT-N* [16,19,20]. In doing so, experimental and theoretical research has followed different paths to build solid bridges between the ever-increasing use of seismic, non-intrusive geophysical methods and the *SPT*, as the *SPT-N* has been widely used for years, both as a design parameter in many geotechnical applications (foundations, liquefaction hazard, slope stability, *etc.*) and as a primary reference to obtain other strength-related soil properties. The approach is quite natural, because both penetration resistance values and shear wave propagation frequencies largely depend on the shear properties of the soil skeleton. Indeed, as will be further explored in this paper, the s-wave velocity, V_s, is strongly influenced by the shear modulus (G), as thoroughly demonstrated in some previous studies [19,21]. For that matter, suitable predictability levels have also been reported in quite a few extensive investigations on correlations between the shear modulus and the *SPT-N* [22], relating at the same time the *SPT-N* and the V_s to the shear elastic properties of the soil.

A comprehensive compilation of previous attempts at developing suitable V_s-*SPT* relations can be found in Thaker and Rao [19], who also proposed their own relationships between V_s (m/s) and uncorrected *SPT-N* blows, summarised in Table 1, based on a historical database composed of 602 data pairs, over which a power-law relationship was fitted.

Moreover, Thaker and Rao [19] discussed an essential question regarding whether the most closely fitted *SPT-N* values for the prediction of V_s should be energy-corrected or otherwise. While some experimental works [23] showed equal fitness levels for both kinds of data, Thaker and Rao [19] recognized a higher level of predictability in the uncorrected *SPT-N* values, so energy corrections were omitted in their expressions, which are summarised in Table 1. These opposing conclusions stress the site-dependent nature of single-variable approaches, in which some important independent variables are left without consideration. For instance, pore water pressure affects the shear strength of a soil, so the correlation fitness will notably vary between saturated and unsaturated soils.

Another comprehensive analysis of V_s-*SPT* relationships was discussed in Ref. [24], who emphasised the discrepancies among some of the conclusions of previous correlations. They highlighted that conclusive results were yet to emerge on the soils, whether fine-grained or cohesionless, that have a greater secondary wave velocity at equal values of *SPT-N*, as different authors had reached different inferences after analysing their empirical results. These opposing results stress the site-dependent character of all the correlations, in which single variable approaches omit significant parameters that might otherwise extend their global scope and applicability.

Some other authors [25–30] have also studied the relationship between V_s - *SPT-N*.

1.1.2. V_p - SPT-N existing correlations

Previous empirical works [31,32] have presented the low correlation coefficients of direct single-variable approaches, as should initially be expected, due to the complex, multi-variable mechanism behind dilatational wave propagation. These analyses should therefore be considered as local studies, heavily dependent upon site conditions. On that point and through a theoretical perspective, Foti [33] pointed out that, mechanically speaking, whereas V_s relies mainly upon the shear modulus, V_p is also quite influenced by both the soil skeleton bulk modulus (K^{SK}) and the water bulk modulus (K^F), thus indicating these dependencies in Eqs. (1) and (2), assuming grain incompressibility and full saturation:

$$V_p = f\left(K^{SK}, G, K^F, n, \rho_s, \rho_F\right) \tag{1}$$

$$V_s = f(G, n, \rho_s, \rho_F) \tag{2}$$

Where n represents porosity, ρ_s particle density, and ρ_F water density.

According to Foti [33], the predictive power of no other factor than V_p should be a low when estimating soil stiffness within these strata -as will be empirically confirmed in Section 2.2 of this paper-, due to the substantial dependence observed in field tests between V_p and water compressibility within saturated layers. Moreover, the pore water content will have a low influence on shear wave velocity [34], to the point of it even being negligible within clayey soils [33].

Furthermore, the wave velocities can also be computed for unsaturated soils [35], introducing five new variables in the case of the V_p, for just one new variable in the case of V_s, which are expressed in Eqs. (3) and (4):

$$V_p = f\left(K^{SK}, G, K^F, n, \rho_s, \rho_F, \upsilon^{SK}, S_r, K^a, \rho_a, m_2^w\right) \tag{3}$$

$$V_s = f(G, n, \rho_s, \rho_F, S_r) \tag{4}$$

Where ν^{SK} is the Poisson's ratio; S_r is the degree of saturation; K^a is the bulk modulus of air; ρ_a is the air density; and m_2^w is the coefficient of water volume change, due to matric suction variations.

1.2. Contents and innovation

These geophysical techniques are quite cost-effective, and several applications might benefit from contrasted and robust correlations such as the one described in this paper, namely the relationship between primary wave velocity and *SPT* results, among which the following three stand out.

- Preliminary geotechnical surveys for predesign and budgetary estimates of foundation costs for projects covering large areas (wind turbine farms, high-speed rail platforms, *etc.*), based on seismic tests performed in as many key locations as needed, with additional *SPT* data at a few of those locations where boreholes are drilled to calibrate the correlation parameters.
- Estimation of soil shear-strength parameters at locations with difficult access, or in environments where probing machinery is seldom available, due either to budgetary restrictions or to regional underdevelopment and a generalized absence of technology.
- Assessment of preliminary soil rippability with the sole use of the *SPT-N*.

Nevertheless, traditional V_s determination through surface-wave modal-dispersion analysis can be a complex task, at times leading to inaccurate estimations of secondary wave velocities [36], while V_p profiles can reflect the actual underground properties of a site with greater accuracy.

Thus, as a feasible alternative for the approaches using the secondary wave velocity, this study will concentrate on a less well travelled path, introducing some new developments on the relationship between primary wave velocity and the *SPT-N*. It will also result in a better understanding of the explanatory potential of the *SPT* regarding the elastic parameters of the soil (namely, soil skeleton and bulk modulus of water, as well as Poisson's ratio).

Furthermore, some recent papers have assessed the multivariable methods as the key to unlocking the next step, seeking to develop universal rather than local correlations between the *SPT-N* and other key parameters, including secondary wave velocity values, which are

Table 1
Correlations between shear wave velocity (V_s [m/s]) and *SPT-N* [19].

Soil type	Correlation	Pearson's coefficient of determination R^2
All soils	$V_s = 59.72 \bullet SPT\text{-}N^{0.42}$	0.77
Sandy soils	$V_s = 51.21 \bullet SPT\text{-}N^{0.45}$	0.78
Clayey soils	$V_s = 62.41 \bullet SPT\text{-}N^{0.42}$	0.78

feasible for both cohesive and cohesionless soils [21].

As dilatational wave propagation has noticeably more parameters than its shear wave counterpart, a multivariable dimensional analysis is suitable. This methodology will provide a good correlation between the V_p and the *SPT-N*, as will be described in Section 3. In that regard, it has been empirically demonstrated that the uncorrected *SPT-N* results produced the most closely fitted relationship with the primary wave velocity, as will subsequently described in Section 2.2.

In view of the relationship between seismic wave velocities and standard penetration resistance, we can outline the main disadvantage of the existing techniques: the limited applicability of single-variable correlations, which fail to capture all the independent variables governing low-strain vibrations and penetration resistance. The use of additional explanatory variables will upgrade the correlations, so that their applicability will be global rather than local.

2. Geotechnical investigation

2.1. Field research

In the course of geotechnical probing of alluvial soils around Juchitán de Zaragoza (a coastal city in the Oaxaca region of Mexico) for the Bii Hioxo Wind Farm, the authors conducted 117 Seismic Refraction tests. Meanwhile, as the geophysical research was performed, the contractor commissioned 117 boreholes on the same spots, right at the centre of each seismic array, thus obtaining a series of continuous Standard Penetration Test profiles for each one. In those tests, their maximum exploration depths ranged from 15 to 30 m and the *SPT-N* was continuously registered every 60 cm. According to the description on the geological map "Juchitán 15–10 D15-1" [37] published by the Geological Mexican Service, the subsoil of the area is formed of alternating clayey and sandy layers of alluvial origin, with different degrees of inter-grain cementation. A geotechnical survey at each of the 23 sites was performed and the main results can be consulted in the following database [38], which includes all the raw data for this investigation.

The Seismic Refraction tests were conducted with a PASI

Fig. 1. Photos during some of the seismic refraction tests: (a) Seismographic acquisition equipment; (b) Geophone; (c) Depiction of the seismic excitation by a sledgehammer impact; (d) Sledgehammer with installed shock detector.

seismograph (Mod. 16S24–P), using a 120 m linear spread of 24 geophones with a natural frequency of 10 Hz and 5 m separation. A 7 kg sledgehammer with a trigger lead-in cable striking a 25 cm × 25 cm steel plate was used as the seismic excitation method. 9 shots spaced 15 m, with a 2.5 m initial and final offsets from the first and last geophones, respectively, were used for each seismic profile (Fig. 1). Each data set, recorded in the SEG-2 format with the PASI Seismograph, was then processed with Rayfract software (Fig. 2).

As the *SPT-N* profiles of the borehole specimens revealed monotonous growth with depth at each test site, it was clearly expected that no hidden layers were missed in the refraction tests (see Fig. 3 for an example).

2.2. Regression-analysis based statistical correlation between SPT-N and V_p

The raw data were analysed using conventional statistical methods, to calculate both the average dilatation wave velocities and the mean *SPT-N* profile values for each probed layer at a confidence level of 95 %. After doing so, the 149 pairs of values were then plotted on *SPT-*V_p graphs for the complete set of soils, regardless of their fines content, and for both clayey and sandy soils, separately (Figs. 4–6). An exponential regression curve was calculated for each scatter plot, thereby indicating the value of the coefficient of determination R^2 in each case.

According to the estimated R^2 values, summarised in Table 2, the goodness of fit of the corrected *SPT-N* values was lower than their raw, uncorrected counterparts, as had previously been observed for the correlation with V_s values [19].

It is also essential to point out that better correlations were found for clayey rather than sandy layers. As most of the sand deposits were fully saturated, if we take into account the importance of the bulk modulus of water in the measured V_p, then the drop in the degree of goodness of fit was consistent with the observed experimental behaviour of these non-cohesive soils.

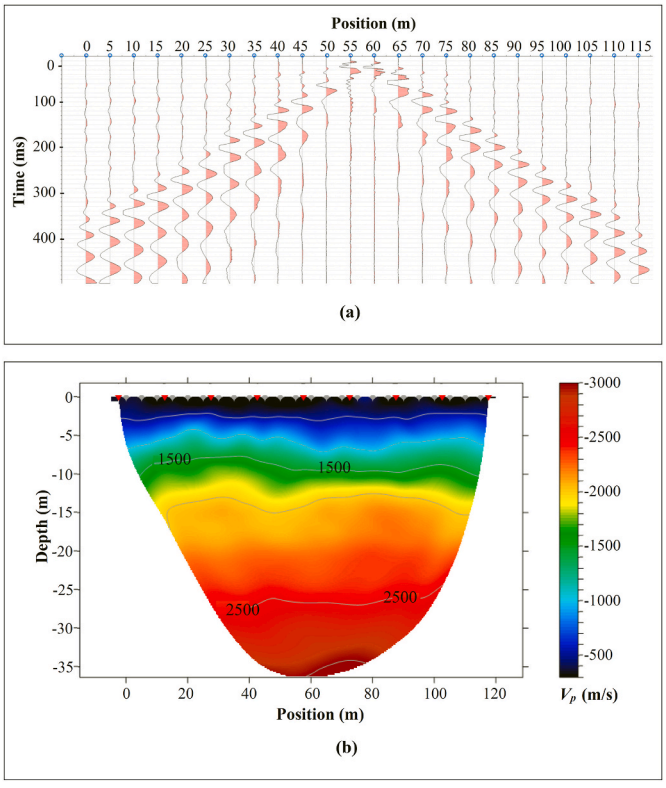

Fig. 2. Example of p-wave profile: (a) before post processing; and (b) after post processing.

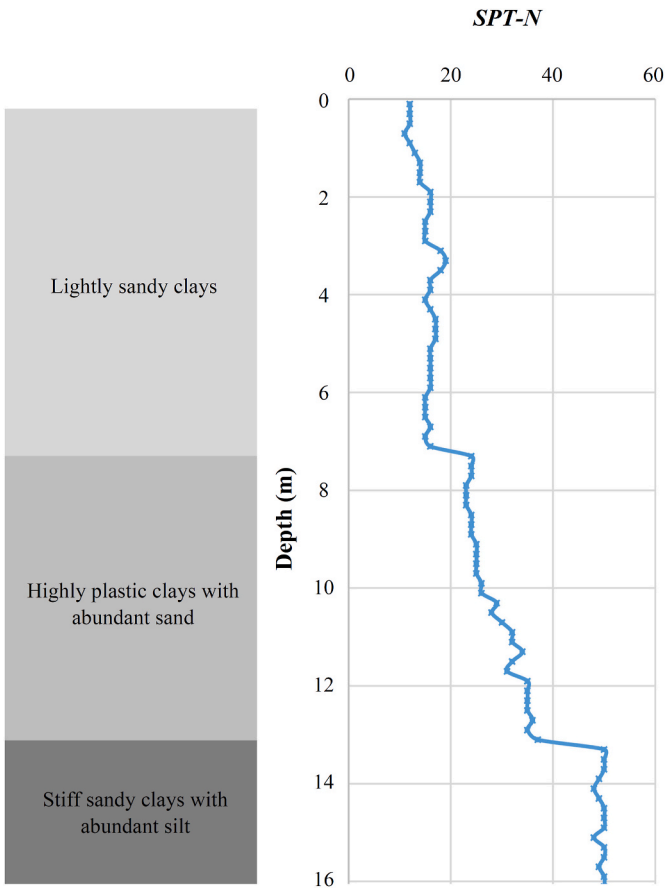

Fig. 3. Example of *SPT-N* profile.

Among the most recent attempts to relate p-wave velocities and *SPT-N*, we may highlight the research of both Ulugergerli and Uyanik [31] and Bery and Saad [32], mentioned in Section 1.1.2.

The former ratified the wide variation range for dilatational wave velocity and the *SPT-N* relationship. Rather than producing a unique statistical regression line to fit their data pairs, the authors developed a lower and an upper boundary (thereby including SPT penetration further away from the usual 50-blow stop value). Their proposed boundaries were:

$$V_p^{upper}(m/s) = 10.008 \cdot ln\, SPT - N + 2193 \quad (5)$$

$$V_p^{lower}(m/s) = 245.97 \cdot \exp^{0.0057 SPT - N} \quad (6)$$

When applied to the current study, those curves satisfactorily enclosed the new data obtained in the present research on alluvial soils, as reflected in Fig. 7.

The latter two authors, Bery and Saad [32], produced an empirical correlation for data pairs obtained from tropical soils and rocks in Sarawak (Malaysia), shown in Eq. (7):

$$V_p(m/s) = 23.605 \cdot SPT - N - 160.43 \quad (7)$$

In Fig. 7, the correlation overlapping the current set of data reveals a linear relationship that is a lower boundary [39] for the alluvial soils investigated in this paper. It emphasises the local scope of this approach, which cannot be properly fitted as a useful global predictive tool.

Completing this section, we must finally mention that another line of research works has been focused on rippability assessment [40]. The author correlated wide ranges of *SPT-N* values with the expected p-wave velocity intervals, indicating that the *SPT* can overcome the limitations of gathering data through seismic refraction tests when soft layers appear below stiffer ones. The reason is that the layer would be missed

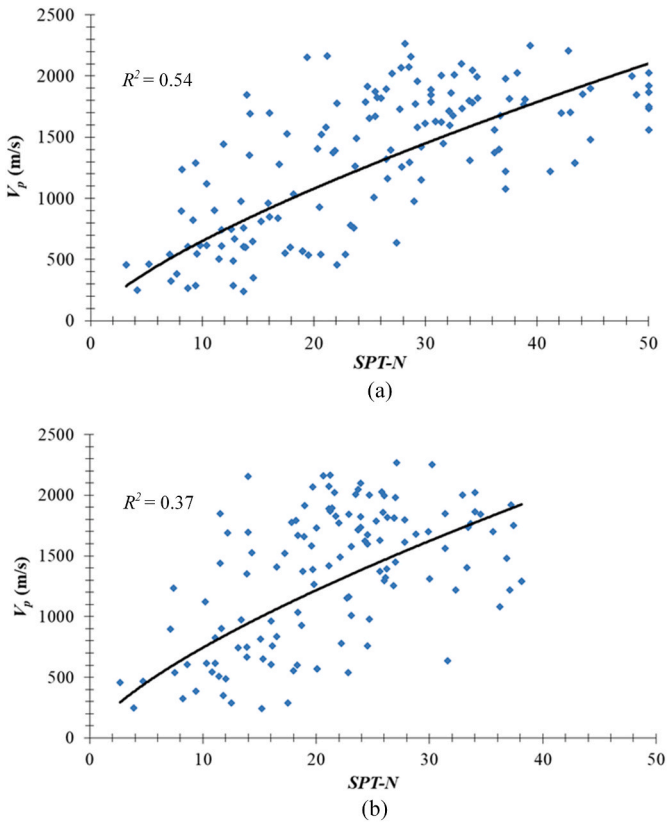

Fig. 4. Correlation between *SPT-N* and V_p (m/s) for all soils: (a) Uncorrected *SPT-N* values; (b) Energy corrected *SPT-N* values.

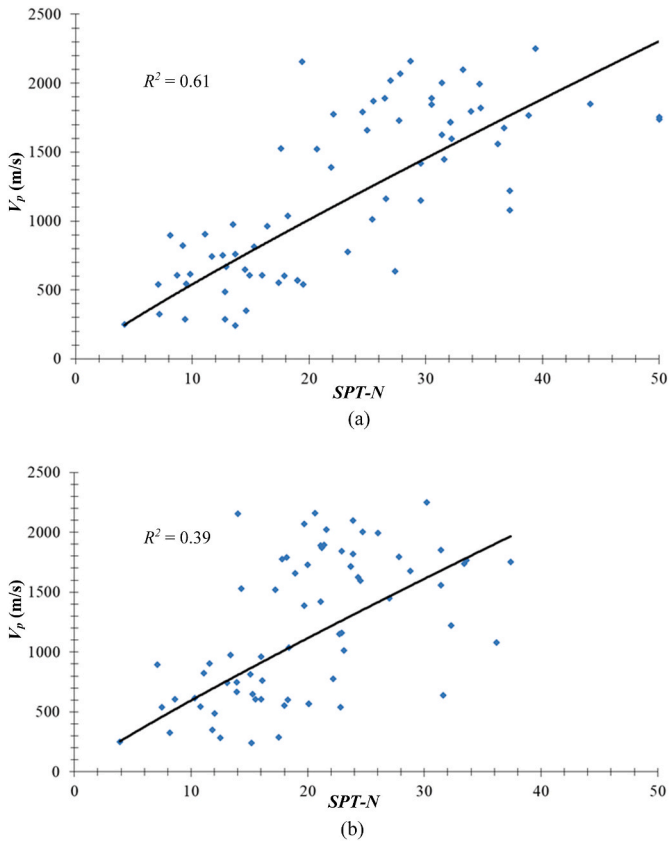

Fig. 5. Correlation between *SPT-N* and V_p (m/s) for clayey soils: (a) Uncorrected *SPT-N* values; (b) Energy corrected *SPT-N* values.

by the seismic profile (hidden layer), but the SPT could certainly register its presence, thus rendering a more complete profile than the geophysical test alone. Nevertheless, the ranges used in that research are quite wide, so its utility is restricted to tentative rippability assessments.

3. Multivariable prediction through dimensional analysis: results and discussion

3.1. Nature of the soils used in the analysis

The extraction of high-quality undisturbed samples of sand layers usually implies the use of non-conventional techniques such as freezing, dewatering, chemical grouting, *etc.* [41–45]. In contrast, traditional sampling devices alter the properties of cohesionless soils, inducing shear strains that change their density and porosity [46–48], which are of paramount importance for a precise multivariable analysis. In this investigation, some alterations were expected in the cohesionless test specimens, because conventional procedures were used to gather the sand samples at the survey locations during a geotechnical field campaign. The scope of the present research was therefore narrowed down to the study of cohesive, clayey layers of soil.

3.2. The Undrained Dilatation Stiffness Index (DSI_u)

A subset of 23 clay layers was sampled before laboratory tests on each layer. In addition to penetration resistance and p-wave velocity, the following properties were in each case measured in the undisturbed specimens: particle density, void ratio, and saturation degree [38]. With the information provided by these parameters, a new multivariable approach was conducted using dimensional analysis.

While dimensional analysis is common in many experimental fields [49–51], it has seldom been used to describe and to predict geotechnical phenomena. Some authors have very recently published studies on this powerful technique that offers promising solutions to various complex, multivariable geotechnical problems [52–55].

As some of the parameters contained in Eq. (3) are rarely obtained in traditional geotechnical surveys, Eq. (8) proposes an alternative definition of the variables upon which the dilatational wave propagation velocity V_p may depend:

$$V_p = f\left(SPT - N, \sigma_v^{'}, p_o, \gamma_s, \gamma_w, e, S_r, g\right) \tag{8}$$

Where ρ'_v is the effective overburden pressure at the centre of the layer where *SPT-N* has been obtained, p_0 is the atmospheric pressure (101.325 kPa), γ_s is the particle specific gravity, γ_w is the water specific gravity, e is the void ratio, and g is the acceleration of gravity.

As the number of different variables amount to n = 9 and the dimensions involved are length [L], mass [M] and time [t], *i.e.*, k = 3, according to Buckingham's p-theorem [56], the n variables can be regrouped into n-k = 9 - 3 = 6 independent dimensionless variables.

Since the p-theorem is a necessary, but not a sufficient [55] condition to generate the dimensionless form of the relationship in Eq. (8), other quantities should be explored, in order to try to obtain the minimum dimensions, regardless of whether they are primary or secondary. However, in this case, the minimum dimensions are k = 3, as it is easy to demonstrate that any other combination of primary and secondary dimensions leads to equal or larger sets of separate dimensions.

The following steps form the non-dimensional variables [55].

1 First, the Q list of the repeated variables of the phenomenon needs to be determined. To do so, Butterfield [55] indicated the convenience of firstly defining a subset R with elements from the original list of variables, V, in Eq. (8), provided that no element is dimensionless or has the same dimensions as the other elements within the subset.

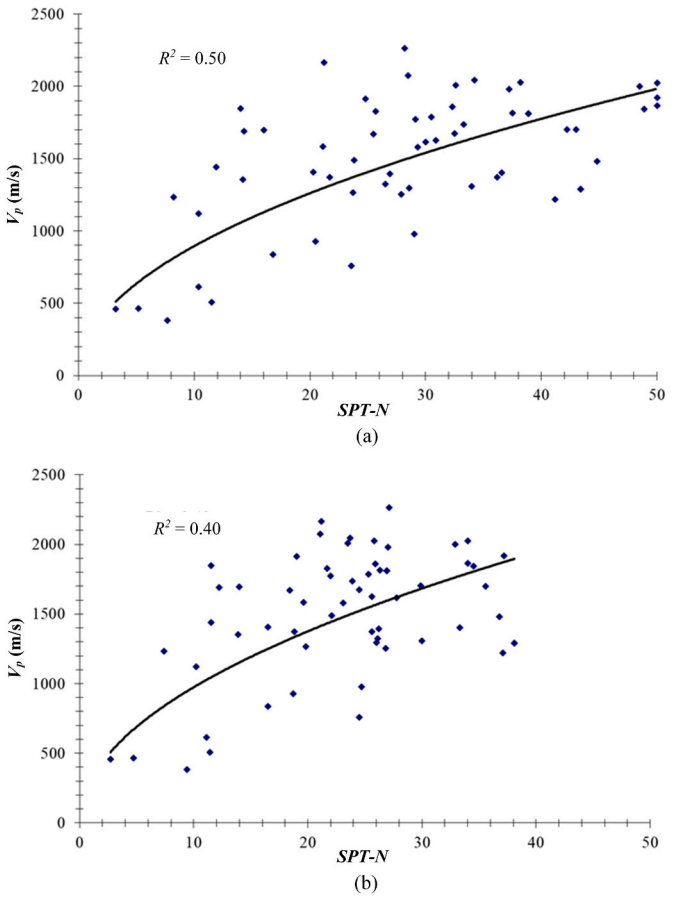

Fig. 6. Correlation between *SPT-N* and V_p (m/s) for sandy soils: (a) Uncorrected *SPT-N* values; (b) Energy corrected *SPT-N* values.

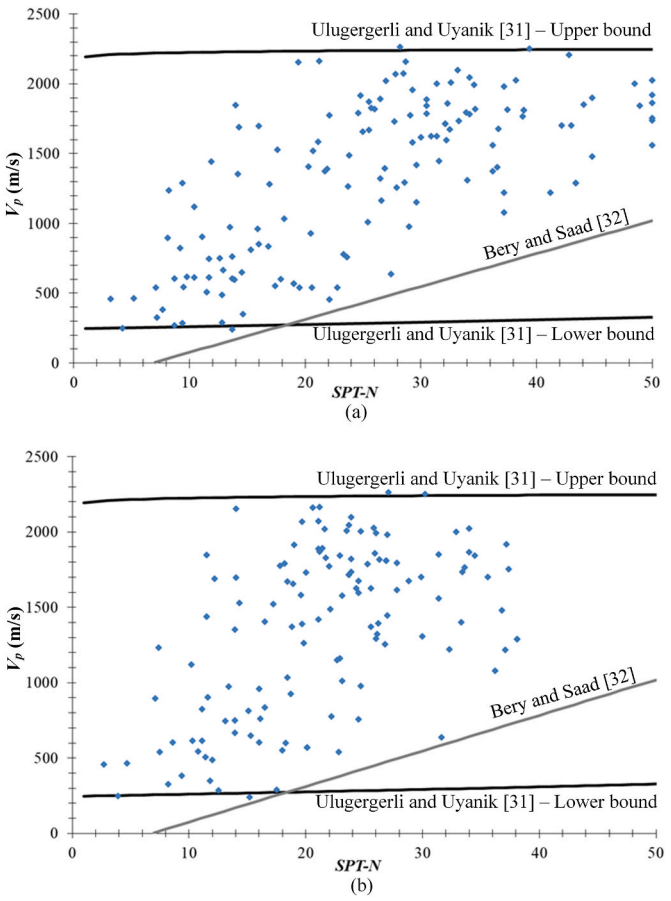

Fig. 7. Upper and lower boundaries as defined by Ulugergerli and Uyanik [31] for all types of soils from the present study and Correlation line for tropical soils and rocks defined by Bery and Saad [32]: (a) uncorrected *SPT-N* values; (b) Energy corrected *SPT-N* values.

Table 2
Correlations between dilatational wave velocity (V_p [m/s]) and *SPT-N*.

SPT-N correction	All soils	Clays	Sands
No correction	$R^2 = 0.54$	$R^2 = 0.61$	$R^2 = 0.50$
Corrected	$R^2 = 0.37$	$R^2 = 0.39$	$R^2 = 0.40$

2 Then, from the R list, a number of k = 3 elements should be chosen to form the Q list, filled with variables that can be repeated in all the dimensional groups.
3 Next, the V-Q list has to be determined, formed of all the isolated variables that can be mixed into a dimensionless variable.
4 The last step is to combine each of the dimensional groups into dimensionless variables.

But before applying the above protocol, the dimensional nature of the *SPT-N* has first to be analysed and defined. It has conventionally been used as a dimensionless index related to the shear strength of a soil. However, due to the penetration procedure, it can also be considered as a measure of the necessary energy to overcome the shear resistance of a given soil within a given cylindrical area. Thus, a "blow" could be considered as a measure of specific work (work per unit area). Both options will be separately studied, to establish whether the dual dimensional/non-dimensional nature of the *SPT* is consistent with a dimensional analysis.

In this section, we will start by considering the *SPT-N* as a dimensionless magnitude. Applying the dimensional analysis protocol, a proposal for a list of variables is shown in Eq. (9) through to (12):

$$V = \left(V_p, SPT-N, \sigma_v^{'}, p_o, \gamma_s, \gamma_w, e, S_r, g\right) \tag{9}$$

$$R = \left(V_p, p_o, \gamma_w, g\right) \tag{10}$$

$$Q = \left(p_o, \gamma_w, g\right) \tag{11}$$

$$V - Q = \left(V_p, SPT-N, \sigma_v^{'}, \gamma_s, e, S_r\right) \tag{12}$$

The final dimensionless relationship is defined below in Eq. (13):

$$\frac{V_p}{\sqrt{\frac{p_o \cdot g}{\gamma_w}}} = f\left(SPT-N, \frac{\sigma_v^{'}}{p_o}, \frac{\gamma_s}{\gamma_w}, e, S_r\right) \tag{13}$$

Following Eq. (13), a new condensed dimensionless variable, the Undrained Dilatation Stiffness Index (DSI_u), is proposed below in Eq. (14):

$$DSI_u = SPT-N^a \cdot \left(\sigma_v^{'}/p_o\right)^b \cdot \left(\gamma_s/\gamma_w\right)^c \cdot e^d \cdot S_r^f \tag{14}$$

where and a, b, c, d, and f are calibration indexes to be adjusted, in order to obtain a satisfactory correlation.

When calibrated, the adjustment shows that $a = b = 2/3$, $c = -5$ and $d = f = -2/3$, and considering $p_0 = 101.325$ kPa, $g = 9.81$ m/s^2 and $\gamma_w = 9.81$ kN/m^3 as constant values, then the dimensionless index, DSI_u, and the relationship between that number and the resulting value of V_p can be expressed in Eqs. (15) and (16) as follows:

$$DSI_u = \frac{\left(\frac{SPT-N}{e \cdot S_r} \cdot \frac{\sigma_v'}{p_o}\right)^{2/3}}{\left(\gamma_s/\gamma_w\right)^5} \quad (15)$$

$$V_p(km/s) = \sqrt{5.07 \cdot DSI_u} \quad (16)$$

The coefficient of determination of Eq. (16) for the 23 sets of analysed data is $R^2 = 0.929$, as can be observed in Fig. 8.

At this point, the statistical accuracy level of the regression can be estimated, using the percent relative error in primary velocity estimation as the main discussion indicator. Table 3 shows both measured and estimated values for primary wave velocity, as well as the percent relative error in its estimation for the 23 sets of data used in this research.

If the percent relative error is plotted against the DSI_u (Fig. 9a) or the measurements of the primary wave velocities (Fig. 9b), we find that the relative error (in absolute values) between estimated and measured values generally falls below 30%. Only one of the data sets yielded higher percent error values after the regression. A normal distribution curve can be assumed for the percent relative error, to understand whether this value can be considered as an outlier (which is consistent with the data, as the frequency distribution chart for the percent error shows a Gaussian trend, as shown in Fig. 10). Thus, as the lower quartile for the distribution of relative errors is $Q_1 = -10.95$ % and the upper one is $Q_3 = 21.15$ % (with the resulting interquartile range $IQR = 32.1$ %), the upper boundary for outliers is $Q_3 + 1.5 \cdot IQR = 69.3$ %. Extracting this outlying set of data from the regression, the correlation shows a robust performance, as this outlier only affects Eq. (16) at the third significant figure of the multiplying factor, 5.07.

It is quite interesting to search for the reason why a few data sets yielded high relative errors when estimating V_p. The authors carefully checked these data, though no errors were found. Some data could be considered as outliers (which must be discarded from the study), as clarified in the preceding paragraph, but some (few) high relative errors were still not considered as outliers. It might very likely mean that there will be more soil variables affecting these correlations than are otherwise considered. Further exploration will be necessary in subsequent investigations, to improve these correlations, through additional variables involved in the process. In any event, the correlations already obtained in this research are very strong ($R^2 = 0.93$), at least enough for most of the geotechnical aims.

Additionally, analysing the dilatational wave prediction deviations with regard to the influence of soil stiffness, it can be observed that the behaviour of the correlation in Eq. (16) is a noticeably good fit for primary wave velocities above 1400 m/s and *SPT-N*>30, as graphically described in Fig. 11, with a predictive error of 6.2 % or less.

3.3. The modified Undrained Dilatation Stiffness Index ($MDSI_u$)

As stated in Section 3.2, the *SPT-N* can be alternatively defined as a measure of work per unit area. In this case, the dimensional analysis protocol leads to the proposal of the four lists of variables described in Eq. (17) through to (19):

$$V = \left(V_p, SPT-N, \sigma_v', p_o, \gamma_s, \gamma_w, e, S_r, g\right) \quad (17)$$

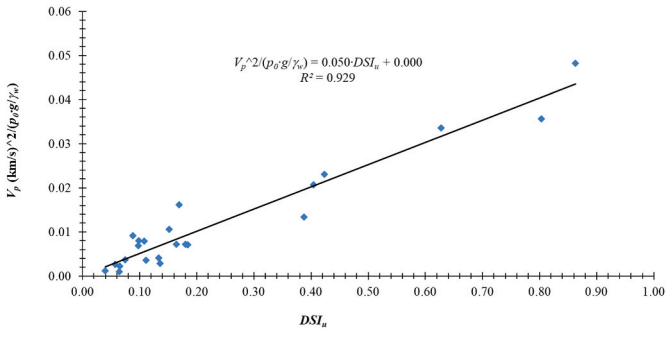

Fig. 8. Correlation between the Undrained Dilatation Stiffness Index (DSI_u) and the dilatational wave velocity value (V_p).

Table 3
Percent relative error in V_p estimation.

V_p (m/s)		Percent relative error
Measured	Estimated	
1162	1402	20.7
904	707	−21.8
1447	1431	−1.1
896	740	−17.4
1528	1464	−4.2
837	703	−16.0
1844	1784	−3.3
1036	876	−15.4
615	616	0.1
326	570	74.9
961	667	−30.5
605	751	24.1
540	830	53.8
357	448	25.5
516	537	4.1
1280	927	−27.6
1900	2018	6.2
850	966	13.7
2209	2092	−5.3
479	574	19.8
851	956	12.3
851	913	7.3
644	823	27.7

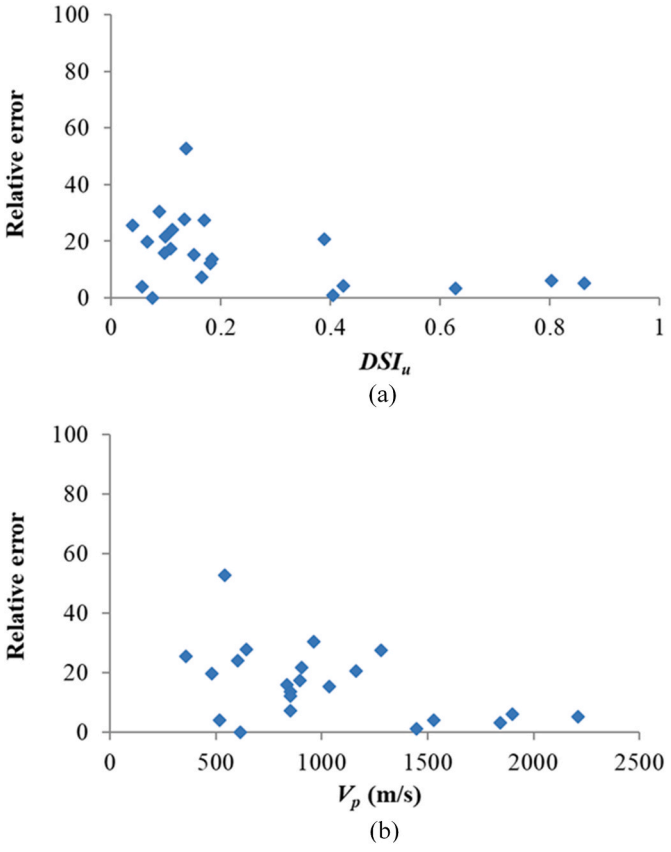

Fig. 9. (A) Percent relative error for V_p estimated values plotted against the DSI_u; and (b) Real V_p measured values.

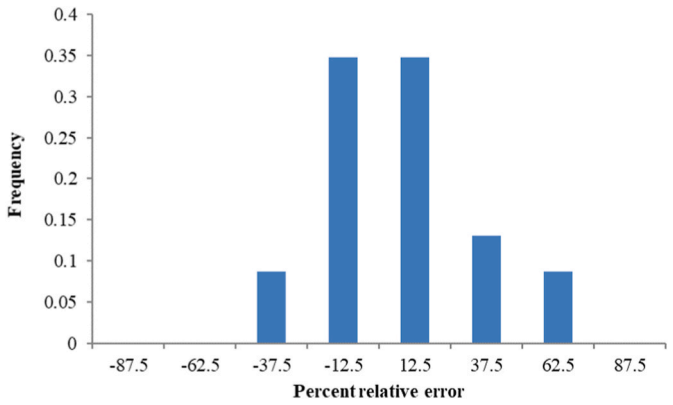

Fig. 10. Frequency distribution chart for the percent relative error in V_p estimations.

$$R = (V_p, SPT-N, p_o, \gamma_w, g) \tag{18}$$

$$Q = (p_o, \gamma_w, g) \tag{19}$$

$$V-Q = (V_p, SPT-N, \sigma_v', \gamma_s, e, S_r) \tag{20}$$

Now, it is easy to see that the original relationship shown in Eq. (8) can finally be defined through the dimensionless expression in Eq. (21):

$$\frac{V_p}{\sqrt{\frac{p_o \cdot g}{\gamma_w}}} = f\left(\frac{SPT-N\cdot\gamma_w}{p_o^2}, \frac{\sigma_v'}{p_o}, \frac{\gamma_s}{\gamma_w}, e, S_r\right) \tag{21}$$

The above should be treated carefully, as the *SPT-N* is a count of "blows", so the units are not homogeneous. The *SPT-N* value must be affected by a conversion factor B [kJ/(m^2·blow)], to produce a suitable equation relating all the magnitudes.

In this case, as all the SPT hammers used during the survey were properly calibrated according to the specified methodology in Ref. [57], the energy transfer ratio (*ETR*) is known for each penetration test. As the theoretical potential specific energy of the *SPT* [58] is 14.4 kJ/(m^2·blow), the conversion factor will be equal to:

$$B\left(kJ/m^2 \cdot blow\right) = 14.4 \cdot ETR \tag{22}$$

Then, the functional dependence in Eq. (21) can be homogenously condensed as a new dimensionless number, the Modified Undrained Dilatation Stiffness Index ($MDSI_u$), which incorporates the conversion factor for the *SPT-N* in each test. Eq. (23) depicts this index:

$$MDSI_u = \left(B\cdot SPT - N\cdot\gamma_w/p_o^2\right)^a \cdot \left(\sigma_v'/p_o\right)^b \cdot \left(\gamma_s/\gamma_w\right)^c \cdot e^d \cdot S_r^f \tag{23}$$

When calibrated, with $a = 1$, $b = 2/3$, $c = -5$, and $d = f = -2/3$, the two final relationships are revealed in Eqs. (24) and (25):

$$MDSI_u = \frac{\left(B\cdot SPT - N\cdot\gamma_w/p_o^2\right)\cdot\left(\frac{1}{e\cdot S_r}\cdot\frac{\sigma_v'}{p_o}\right)^{2/3}}{\left(\gamma_s/\gamma_w\right)^5} \tag{24}$$

$$V_p(km/s) = \sqrt{618.11\cdot MDSI_u} \tag{25}$$

For Eq. (24), the determination coefficient is $R^2 = 0.925$, and the relationship between V_p and $MDSI_u$ is plotted in Fig. 12, while the percent relative errors are slightly above those of the regression with the DSI_u, as can be seen in Figs. 9 and 13. As happened with the regression based on the DSI_u, for primary wave velocity values above 1400 m/s and for *SPT-N* blow-counts above 30, the predictive capability of the regression increases, as graphically shown in Fig. 14.

While Eq. (25) renders a similar fitness as Eq. (16), the use of the $MDSI_u$ has a potential advantage over the DSI_u: as the $MDSI_u$ depends on the specific work of the penetration test, it can be adapted to other types of probing devices, by means of a proper selection of the conversion

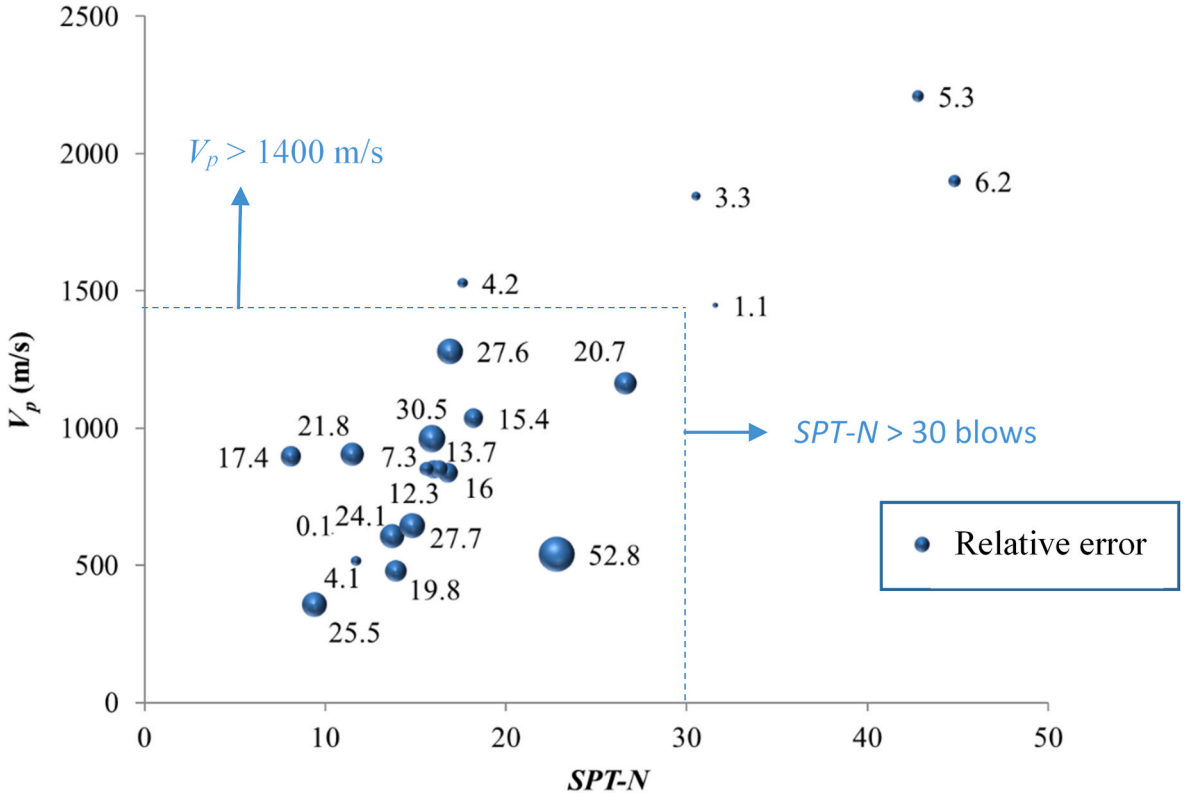

Fig. 11. Percent V_p relative error plotted simultaneously against the primary wave velocity V_p and *SPT-N* without outliers for the regression with DSI_u.

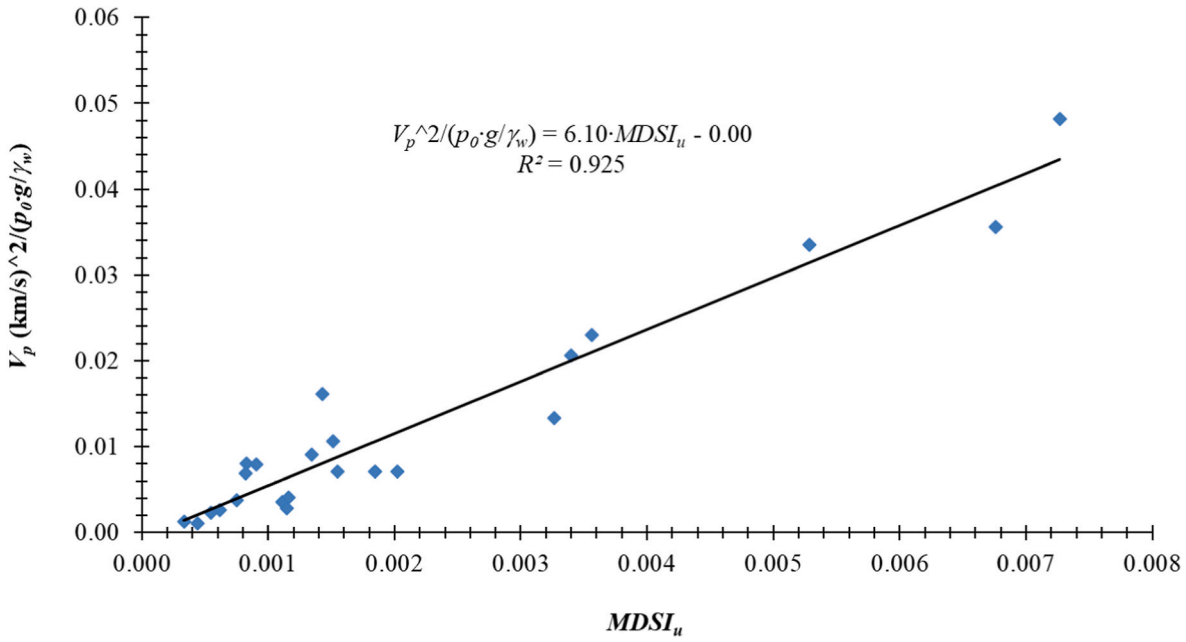

Fig. 12. Correlation between the Modified Undrained Dilatation Stiffness Index ($MDSI_u$) and the dilatational wave velocity (V_p) values.

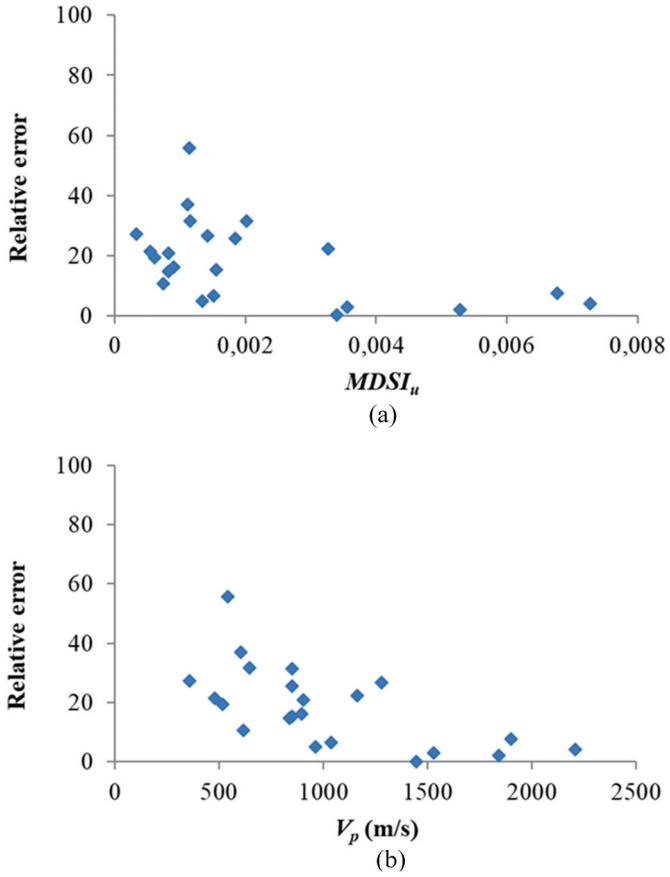

Fig. 13. Percent relative error for V_p estimated values plotted against (a) $MDSI_u$; and b) the primary velocity measured values.

factor.

Further tests should be carried out to study whether the conversion factor could enhance the explanatory power of the penetration blow count, not only for the *SPT* but, also, for other penetration tests, as the specific work per blow is a common way of expressing the energy delivered with each fall of the hammer of any given probing apparatus. In fact, the specific nominal work per blow for each probing apparatus is specified in Ref. [59]. All the work-per-blow values are summarised below in Table 4.

These values should be adjusted by their own conversion factors, depending on the given *ETR* calibrations, and then computed using new regression correlations with the $MDSI_u$ number.

4. Conclusions

The impracticalities of the few current correlations between V_p and *SPT-N* have been demonstrated in this research. Ulugergerli and Uyanik [31] proposed some that have been proven to fit our research data quite well, but their correlations only define lower and upper bounds. And Bery and Saad [32] proposed a correlation that behaves as a lower boundary and that is likely only a robust correlation for local data.

Robust new relationships (R^2 = 0.93) between V_p and *SPT-N* have been obtained (see Eqs. (15), (16), (24) and (25)) through a multivariable dimensional analysis, also involving other soil parameters (e, S_r, σ'_v and γ_s).

Statistical uncertainty analysis has shown that the predictive capability of this proposed method for correlating V_p and *SPT-N* increases with soil stiffness.

If *SPT-N* is defined as a measure of work per unit area, then the results (with only slightly higher error levels) are similar to those produced when considering *SPT-N* as a dimensionless magnitude, although that can help to correlate V_p not only to *SPT* tests, but also to any other kind of penetration test.

Author statement

All authors contributed equally at all stages of the manuscript.

Declaration of competing interest

The authors declare that they have no known competing financial interests or personal relationships that could have appeared to influence the work reported in this paper.

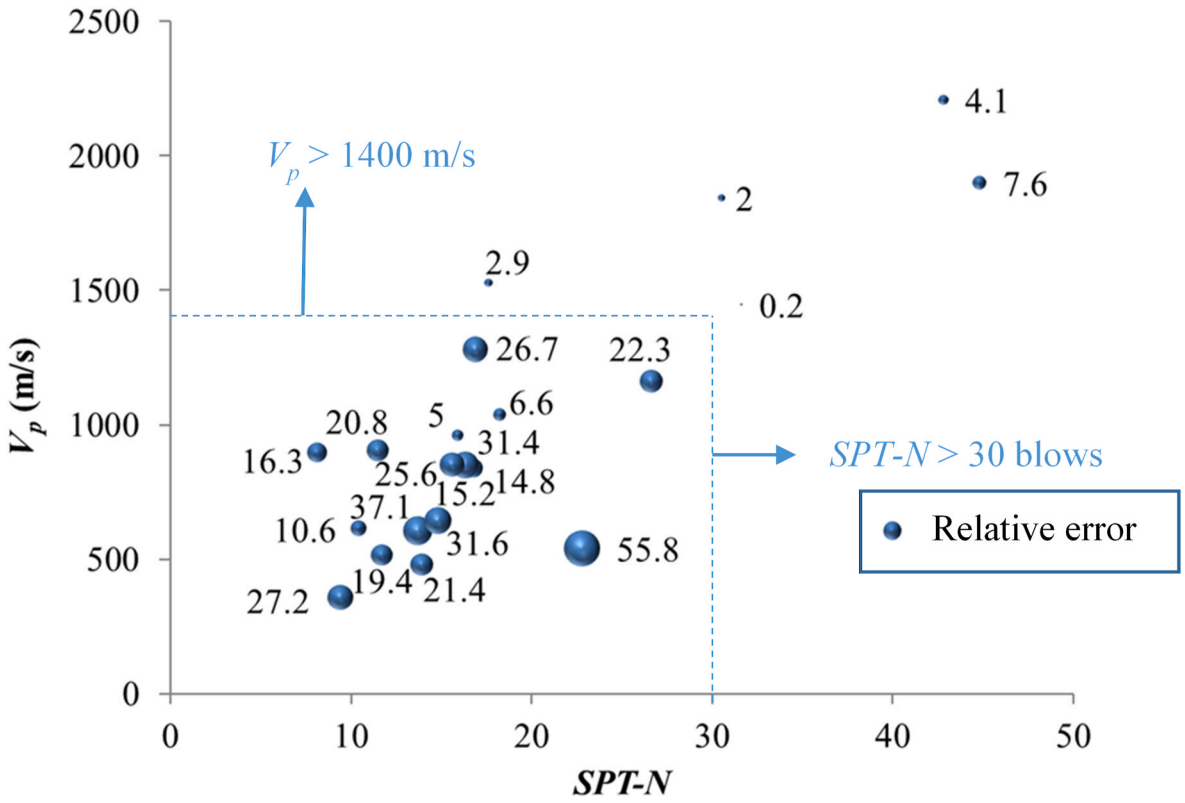

Fig. 14. Percent V_p relative error plotted simultaneously against the primary wave velocity V_p and *SPT-N* without outliers for the regression with $MDSI_u$.

Table 4
Specific work per blow for different probing devices [59].

Probing device	Specific nominal work per blow (kJ/m^2·blow)
DPL (Deep Probe - Light)	50
DPM (Deep Probe - Medium)	100
DPH (Deep Probe - Heavy)	167
DPSH-A (Deep Probe - Super Heavy A)	194
DPSH-B (Deep Probe - Super Heavy B)	238

Data availability

I have shared the link to my data/code at the "Attach File step"
New correlations between Vp and SPT-N-Research data (Original data) (Mendeley Data)

Acknowledgements

The authors would like to express their thanks and recognition to the staff at MS Enertech for providing the borehole logs and laboratory tests reports analysed in this document and, also, for making possible the logistical support and access to the sites where the geophysical tests have been performed.

References

[1] Foti S, Lai CG, Rix GJ, Strobbia C. Surface wave methods for near-surface site characterization. first ed. Boca Raton, FL: CRC press; 2014.
[2] Milsom J, Eriksen A. Field geophysics. first ed. Denver: EEGS; 2013.
[3] Dal Moro G. Surface wave analysis for near surface applications. first ed. Oxford: Elsevier; 2014.
[4] Hettiarachchi H, Brown T. Use of SPT blow counts to estimate shear strength properties of soils: energy balance approach. J Geotech Geoenviron Eng 2009;135:830–4. https://doi.org/10.1061/(ASCE)GT.1943-5606.0000016.
[5] Shooshpasha I, Mola-Abasi H, Jamalian A, Dikmen Ü, Salahi M. Validation and application of empirical shear wave velocity models based on standard penetration test. Comput Methods Civ Eng 2013;4:25.
[6] Hatanaka M, Uchida A. Empirical correlation between penetration resistance and internal friction angle of sandy soils. Soils Found 1996;36:1–10. https://doi.org/10.3208/sandf.36.4_1.
[7] Kulhawy FH, Mayne PW. Manual on estimating soil properties for foundation design. In: Geotechnical engineering group. first ed. Ithaca, New York: Cornell University; 1990.
[8] Peck RB, Hanson WE, Thornburn TH. Foundation engineering. second ed. New York: John Wiley & Sons; 1991.
[9] Cubrinovski M, Ishihara K. Correlation between penetration resistance and relative density of sandy soils. In: Proceedings of the fifteenth international conference on soil mechanics and geotechnical engineering, vols. 1–3. Leiden: A a Balkema Publishers; 2001. p. 393–6.
[10] Gibbs HJ, Holtz WG. Research on determining the density of sands by spoon penetration testing. In: Proceedings of the 4th international conference on soil mechanics; 1957. p. 35–9. London.
[11] Skempton AW. Standard Penetration Test procedures and the effects in sands of overburden pressure, relative density, particle-size, aging and overconsolidation. Geotechnique 1986;36:425–47. https://doi.org/10.1680/geot.1986.36.3.425.
[12] Sanglerat G. The penetrometer and soil exploration: interpretation of penetration diagrams - theory and practice. first ed. Amsterdam: Elsevier Pub. Co.; 1972.
[13] Terzaghi K, Peck RB. Soil mechanics in engineering practice. Hoboken, New Jersey: John Wiley & Sons Inc; 1967.
[14] Sowers GF, Sowers GB. Introductory soil mechanics and foundations: geotechnical engineering. fourth ed. London: Pearson College Div; 1979.
[15] Stroud MA. The Standard Penetration Test in insensitive clays an soft rocks. In: Proceedings of the 1st European symposium on penetration testing; 1974. p. 367–75. Stockholm, Sweden.
[16] Mayne PW, Christopher BR, DeJong J. Manual on subsurface investigations. first ed. Washington: National Highway Institute; 2001.
[17] Sivrikaya O. Comparison of Artificial Neural Networks models with correlative works on undrained shear strength. Eurasian Soil Sci 2009;42:1487–96. https://doi.org/10.1134/S1064229309130092.
[18] Abdulabbas Aab YK. Estimation of shear strength parameters of soils using ANN technique. Int J Civ Struct Environ Infrastruct Eng Res Dev 2014;4:1–10.
[19] Thaker TP, Rao KS. Development of statistical correlations between shear wave velocity and penetration resistance using MASW technique. In: 2011 pan-Am CGS geotechnical conference. Toronto, Ontario: Canada; 2011.

[20] Dikmen Ü. Statistical correlations of shear wave velocity and penetration resistance for soils. J Geophys Eng 2009;6:61–72. https://doi.org/10.1088/1742-2132/6/1/007.
[21] Akin MK, Kramer SL, Topal T. Empirical correlations of shear wave velocity (V_s) and penetration resistance (SPT-N) for different soils in an earthquake-prone area (Erbaa-Turkey). Eng Geol 2011;119:1–17. https://doi.org/10.1016/j.enggeo.2011.01.007.
[22] Anbazhagan P, Parihar A, Rashmi HN. Review of correlations between SPT N and shear modulus: a new correlation applicable to any region. Soil Dynam Earthq Eng 2012;36:52–69. https://doi.org/10.1016/j.soildyn.2012.01.005.
[23] Maheshwari BK, Mahajan AK, Sharma ML, Paul DK, Kaynia AM, Lindholm C. Relationship between shear wave velocity and SPT resistance for sandy soils in the ganga basin. Int J Geotech Eng 2013;7:60–6. https://doi.org/10.1179/1938636212Z.0000000007.
[24] Marto A, Soon TC, Kasim F, Suhatril M. A correlation of shear wave velocity and standard penetration resistance. Electron J Geotech Eng 2013;18:463–71.
[25] Bang E-S, Kim D-S. Evaluation of shear wave velocity profile using SPT based uphole method. Soil Dynam Earthq Eng 2007;27:741–58. https://doi.org/10.1016/j.soildyn.2006.12.004.
[26] Fabbrocino S, Lanzano G, Forte G, de Magistris FS, Fabbrocino G. SPT blow count vs. shear wave velocity relationship in the structurally complex formations of the Molise Region (Italy). Eng Geol 2015;187:84–97. https://doi.org/10.1016/j.enggeo.2014.12.016.
[27] Kirar B, Maheshwari BK, Muley P. Correlation between shear wave velocity (v_s) and SPT resistance (N) for roorkee region. Int J Geosynth Ground Eng 2016;2. https://doi.org/10.1007/s40891-016-0047-5.
[28] Lu C-C, Hwang J-H. Correlations between vs and SPT-N by different borehole measurement methods: effect on seismic site classification. Bull Earthq Eng 2020;18:1139–59. https://doi.org/10.1007/s10518-019-00767-1.
[29] Rahimi S, Wood CM, Wotherspoon LM. Influence of soil aging on SPT-V_s correlation and seismic site classification. Eng Geol 2020;272. https://doi.org/10.1016/j.enggeo.2020.105653.
[30] Sun C-G, Cho C-S, Son M, Shin JS. Correlations between shear wave velocity and in-situ penetration test results for Korean soil deposits. Pure Appl Geophys 2013;170:271–81. https://doi.org/10.1007/s00024-012-0516-2.
[31] Ulugergerli EU, Uyanik O. Statistical correlations between seismic wave velocities and SPT blow counts and the relative density of soils. J Test Eval 2006;35:187–91.
[32] Bery AA, Saad R. Correlation of seismic P-wave velocities with engineering parameters (N value and rock quality) for tropical environmental study. Int J Geosci 2012;3:749–57. https://doi.org/10.4236/ijg.2012.34075.
[33] Foti S. Combined use of geophysical methods in site characterization. In: Roberto Quental Coutinho PWM, editor. Geotechnical and geophysical site characterization 4, porto de Galinhas. Brazil: CRC Press; 2012. p. 43–61.
[34] Qiu T, Fox P. Effective soil density for small strain shear wave propagation. In: Geotechnical earthquake engineering and soil dynamics IV; 2008. p. 1–9. Sacramento.
[35] Conte E, Cosentini RM, Troncone A. Shear and dilatational wave velocities for unsaturated soils. Soil Dynam Earthq Eng 2009;29:946–52. https://doi.org/10.1016/j.soildyn.2008.11.001.
[36] Dal Moro G, Moura RMM, Moustafa SSR. Multi-component joint analysis of surface waves. J Appl Geophys 2015;119:128–38. https://doi.org/10.1016/j.jappgeo.2015.05.014.
[37] Mexican Geological Service. Juchitan 2000;15–10 D15–1.
[38] Ortiz-Palacio S, Ibanez SJ, Sancho D, Porres JA. New correlations between V_p and SPT-N-research data, vol. 1. Mendeley Data; 2023. https://doi.org/10.17632/555wg7w63x.1.
[39] Ibanez SJ, Ortiz-Palacio S, Lopez-Ausin V, Porres-Benito JA. Correlation of p-wave velocity and SPT-N on volcanic soils in Costa Rica. In: Proceedings of the 5th international conference on geotechnical and geophysical site characterisation. Gold Coast, Australia: ISC 2016; 2016. p. 323–7.
[40] Tsang K-m. Relationship between P-wave velocity & SPT N values and application toassessment of excavatability of terrain. Hong Kong: University of Hong Kong; 2004. https://doi.org/10.5353/th_b4309455. Pokfulam, Hong Kong SAR, HKU Theses Online (HKUTO).
[41] Dickinson GRE. The undisturbed sampling of saturated cohesionless soil using A gelatin injection technique. Hamilton, Ontario, Canada: Open Access Dissertations and Theses; 1975.
[42] Singh S, Seed HB, Chan C. Undisturbed sampling of saturated sands by freezing. J Geotech Geoenviron Eng 1982;108. https://doi.org/10.1061/AJGEB6.0001242.
[43] Marcuson WF, Franklin AG. State of the art of undisturbed sampling of cohesionless soils. first ed. Washington: DTIC Document; 1979.
[44] Windisch SJ, Soulié M. Technique for study of granular materials. J Soil Mech Found Div 1970;97. https://doi.org/10.1061/JSFEAQ.0001430.
[45] Barton CM. Bore hole sampling of saturated uncemented sands and gravels. Ground Water 1974;12:170–81. https://doi.org/10.1111/j.1745-6584.1974.tb03017.x.
[46] Castro G. Liquefaction and cyclic mobility of saturated sands. J Geotech Eng Div 1975;101:551–69. https://doi.org/10.1061/AJGEB6.0000173.
[47] Seed HB, Singh S, Chan C. Considerations in undisturbed sampling of sands. J Geotech Geoenviron Eng 1982;108. https://doi.org/10.1061/AJGEB6.0001243.
[48] Griffin DF. Errors in-place density and its role in geotechnical projects involving cohesionless soils. In: ASTM International, editor. Evaluation of relative density and its role in geotechnical projects involving cohesionless soils: a symposium presented at the 75th annual meeting. Los Angeles: American Society for Testing & Materials; 1973. p. 510.
[49] Sonin AA. The physical basis of dimensional analysis. second ed. Massachusetts, Cambridge, MA: Massachusetts Institute of Technology; 2001.
[50] Kuneš J. Similarity and modeling in science and engineering. first ed. Cambridge: Cambridge International Science Publishing Limited; 2012.
[51] Dimitrakopoulos E, Kappos AJ, Makris N. Dimensional analysis of yielding and pounding structures for records without distinct pulses. Soil Dynam Earthq Eng 2009;29:1170–80. https://doi.org/10.1016/j.soildyn.2009.02.006.
[52] Muir Wood D. Geotechnical modelling. first ed. London: Taylor & Francis; 2003.
[53] Arunachalam AVM. Application of dimensional analysis to estimation of ice-induced pressures on rigid vertical structures. Can J Civ Eng 2005;32:968–80. https://doi.org/10.1139/l05-047.
[54] Buzzi O. On the use of dimensional analysis to predict swelling strain. Eng Geol 2010;116:149–56. https://doi.org/10.1016/j.enggeo.2010.08.005.
[55] Butterfield R. Dimensional analysis for geotechnical engineers. Geotechnique 1999;49:357–66. https://doi.org/10.1680/geot.1999.49.3.357.
[56] Buckingham E. On physically similar systems; illustrations of the use of dimensional equations. Phys Rev 1914;4:345–76. https://doi.org/10.1103/PhysRev.4.345.
[57] ASTM. D 4633-10. Standard test method for energy measurement for dynamic penetrometers. West Conshohocken, PA: ASTM International; 2010.
[58] ASTM. D 1586-11. Standard test method for standard penetration test (SPT) and split-barrel sampling of soils. West Conshohocken, PA: ASTM International; 2011.
[59] CEN. EN ISO 22476-2. Geotechnical investigation and testing - field testing - Part 2: dynamic probing. Brussels, Belgium: European Committee for Standardisation; 2005.